Structure and Mechanical Characteristics of Ti₂AlC MAX Phase Cathodes and Deposited Ion-Plasma Coatings

M.A. Bortnitskaya[1], E.N. Reshetnyak[1], A.S. Kuprin[1], T.A. Prikhna[2], V.B. Sverdun[2], I.V. Kolodiy[1],
V.A. Belous[1], V.G. Marinin[1], T.B. Serbenyuk[2]

[1] *National Science Center "Kharkiv Institute of Physics and Technology", 1, Akademichna St.,
61108 Kharkiv, Ukraine*
[2] *V.N. Bakul Institute for Superhard Materials of the National Academy of Sciences of Ukraine,
2, Avtozavods'ka St., 04074 Kyiv, Ukraine*

In this work, the characteristics of the structure, hardness, elasticity, and cavitation resistance of the material of Ti₂AlC MAX phase cathodes manufactured by hot pressing, as well as ion-plasma coatings deposited using these cathodes on titanium alloy Ti6Al4V, have been studied. It was found that the cathode material, which contains 83 wt. % MAX phase Ti₂AlC, is characterized by a hardness of 10 GPa, a *H/E* value of 0.04, and low cavitation resistance. The average cavitation wear of the cathode is 4 times higher than that of the titanium alloy Ti6Al4V. It was found that the elemental and phase composition of the obtained coatings differs from the composition of the cathode. The main phase in the coatings is nanocrystalline carbide (Ti, Al) C with a cubic structure of the NaCl type. $Ti_{0.58}Al_{0.17}C_{0.25}$ coatings deposited by ion sputtering using an arc gas plasma source are characterized by a hardness of 21 GPa. The hardness of vacuum-arc coating $Ti_{0.65}Al_{0.07}C_{0.28}$ is closer to the hardness of the cathode – 13 GPa, which is due to the presence of *a*-Ti in its composition. The *H/E* ratio of the coatings is 1.5 times higher than that of the cathode, which is a prerequisite for high cavitation resistance. The average rate of cavitation wear of vacuum arc coating $Ti_{0.65}Al_{0.07}C_{0.28}$ is 1.5 times lower than that of the vacuum arc coating TiN and 3 times lower than that of the uncoated Ti6Al4V alloy.

Keywords: MAX phase, Coatings, Vacuum-arc deposition, Ion sputtering, Nanoindentation, Cavitation wear.

1. INTRODUCTION

The development of new lightweight, durable and heat-resistant materials that meet the modern requirements of designers of energy and transport systems is the most important task of materials science. In recent years, interest has increased in MAX phases – a new class of ternary refractory compounds possessing a unique combination of properties of metals and ceramics, which is due to their special crystal structure. MAX phases correspond to the formula $M_{n+1}AX_n$ with a hexagonal close packing, where M is a transition metal, A is an element of the A-subgroup of the periodic table, X is carbon or nitrogen. They are natural nanolaminates, have a layered crystal structure, in which carbide or nitride blocks $[M_{n+1}X_n]$ are separated by monolayers of atoms of the elements of IIIA and IVA groups [1].

Among the many MAX phases synthesized to date, titanium-based MAX phases are of great interest: Ti₂AlC, Ti₂AlN, Ti₃AlC₂ and Ti₃SiC₂. They have high electrical and thermal conductivity, low coefficient of friction, high rigidity, high resistance to damage, high temperature resistance, high resistance to oxidation and thermal shock. The resistance of MAX phases to cyclic loads at temperatures above 1000 °C is not inferior and often exceeds the resistance of most known heat-resistant materials. Ti₂AlC MAX phase has attracted attention because of its stability at temperatures up to 1400 °C. This property stems from the formation of a protective Al₂O₃ layer, which has a thermal expansion coefficient comparable to that of the MAX phase itself [2]. Together with a low specific weight,

these properties of Ti₂AlC open up broad prospects for application in various industries. It is believed that MAX phases based on titanium can find application in the production of turbines, engines and pumps, including as a material for protective coatings on the surface of titanium alloy parts exposed to intense thermal, chemical, and mechanical stress [3]. This dictates the need to obtain quantitative data on the resistance of MAX phases and coatings based on them to various types of wear, in particular, under conditions of micro-impacts created by cavitation in various media.

Most of the bulk-form MAX phase was synthesized using hot isostatic pressing (HIP) [4] and spark plasma sintering (SPS) [5] by sintering a mixed powder of elements or compounds at a very high temperature. The properties of the obtained materials strongly depend on the percentage of MAX phase and their final porosity. The work [6] shows the possibility of obtaining dense (up to 99 %) polycrystalline samples of MAX phases of the Ti-Al-C system by hot pressing of mixtures of Ti, TiC, and Al powders preliminarily sintered in an argon atmosphere. The workpieces obtained in this way can be used for the manufacture of both machine parts and targets or cathodes that make it possible to synthesize thin films and coatings based on MAX phases.

To obtain coatings based on MAX phases, various methods of physical deposition are used, such as magnetron sputtering, cathodic arc deposition, and pulsed laser deposition [7]. Until now, most often Ti₂AlC coatings were obtained by magnetron deposition [8]. The required ratio of atoms of elements in coatings Ti:Al:C = 2:1:1 was achieved using three single-element Ti, Al

and C targets, applying different power to them [9-11]. Sputtering only one three-component target of the required composition can simplify the deposition process. However, during magnetron sputtering of such a target, it is not always possible to ensure the reproducibility of the elemental composition of the cathode, and the ratio of the components in the coatings may differ from the stoichiometric ratio for the MAX phase [12, 13]. In this regard, it is of interest to test various ion-plasma deposition methods of coatings using a single multicomponent cathode based on the MAX phase.

The aim of this work was to study the structure, characteristics of hardness, elasticity and cavitation resistance of the cathode based on Ti_2AlC MAX phase manufactured by hot pressing. With its help, we also studied the composition, structure and properties of ion-plasma coatings deposited on substrates of titanium alloy Ti6Al4V. Two methods of obtaining coatings have been implemented: vacuum-arc deposition and ion sputtering using an arc gas plasma source.

2. EXPERIMENTAL TECHNIQUE

Cathodes based on Ti_2AlC MAX phase in the form of discs 60 mm in diameter and 5 mm thick were produced by the following single-stage technology: hot pressing of TiH_2, TiC and Al powders under a pressure of 30 MPa at 1350 °C for 30 min [14]. To study the structure and properties of the cathode material, specimens 20×20×10 mm in size were cut from it. The cathode mandrel for vacuum arc deposition was made of VT1-0 titanium alloy.

The cathodes were used for the deposition of ion-plasma coatings in two ways: vacuum-arc deposition and ion sputtering of the cathode using an arc gas plasma source. In the first case, vacuum-arc coatings were deposited on a Bulat installation with a system for magnetic retention of the cathode spot [15]. The vacuum-arc discharge was generated at the cathode based on Ti_2AlC MAX phase at a residual pressure in the vacuum chamber of $\sim 10^{-3}$ Pa. The discharge current was 60 A. A negative bias potential of 100 V was applied to the substrate located at a distance of 25 cm from the cathode.

For deposition of coatings by the second method, an arc gas plasma source with a tungsten hot cathode was used. [16]. Preliminary evacuation of the setup was carried out until the vacuum in the chamber was at least 10^{-3} Pa. The sputtering of the cathode (target) based on Ti_2AlC MAX phase was carried out by gas ions extracted from the discharge plasma when a negative potential was applied. Ar was used as a working gas at a pressure of 0.8 Pa. The experiments were carried out at a positive anode potential of 50 V and a discharge current of 20 A. The distance between the anode and cathode from Ti_2AlC MAX phase was 100 mm, the ion current density was 15 mA/cm², and the sputtering potential at the cathode was 1000 V. A negative bias potential of 50 V was applied to the substrate located at a distance of 5 cm from the cathode.

Coatings ~ 10 μm thick were deposited on polished Ti6Al4V alloy substrates in the form of disks 12 mm in diameter and 5 mm thick. The surface morphology and cross-section of the coatings were studied using a JSM-

7001F scanning electron microscope. The elemental composition of the cathode and coatings was monitored by X-ray fluorescence analysis on a Sprut-VM spectrometer, as well as by energy dispersive spectroscopy on a JSM-7001F scanning electron microscope.

X-ray structural analysis of the cathode and coatings was carried out on a DRON-4-07 diffractometer in Cu-Kα radiation using a selectively absorbing nickel filter. Phase analysis of the samples and determination of the crystal lattice parameters of the identified phases were carried out using the Rietveld method. The size (*L*) of crystallites (coherent diffraction domains) in the coatings was calculated from the Scherrer formula.

The hardness (*H*) and Young's modulus (*E*) of the cathode and coatings were determined using a Nano Indenter G200 nanohardness tester (MTS Systems, United States) with a Berkovich diamond indenter in the form of a trihedral pyramid. The continuous stiffness measurement (CSM) method was used. This method allows continuous measurement of the contact stiffness, which ensures continuous measurement of *E* and *H* values during the indenter penetration [17]. Ten prints were applied to each sample and then the results were averaged.

The cavitation wear of the samples was investigated at the stand described in [18]. The cavitation zone was formed below the end surface of the concentrator mounted in a distilled water vessel at a distance of 0.5 ± 0.05 mm from the sample surface. The vibration amplitude of the end surface of the concentrator is 30 ± 2 μm at a frequency of 20 kHz [19]. Cavitation wear was determined by mass loss of the samples with an accuracy of ± 0.015 mg.

3. RESULTS AND DISCUSSION

In Fig. 1a, a photo of one of the obtained cathodes is shown. The cathode surface is smooth, dense and uniform. X-ray diffraction analysis indicates that the used hot-pressing method provides a material based on Ti_2AlC MAX phase. The diffractogram of the cathode is shown in Fig. 2, and the results of the phase analysis are in Table 1. Three phases were revealed in the cathode. The main one is Ti_2AlC MAX phase (hexagonal system) with a weight content of 83 wt. %. In addition, the sample contains graphite C (hexagonal system) with a weight content of 14 wt. % and titanium carbide TiC (cubic system) with a weight content of 3 wt. %. The crystal lattice parameters of the identified phases are quite close to the tabulated values. The results of the elemental analysis of the cathode surface are also shown in Table 1. The atomic ratio of titanium and aluminum in the surface layer of the cathode is Ti:Al = 2.8: 1.

Tests of the performance of the cathode based on Ti_2AlC MAX phase during vacuum-arc synthesis of the coatings indicate that the cathode operates stably and provides a sufficiently high deposition rate of vacuum arc coatings up to 5 μm/h. However, visual inspection of the cathode after 3 h of testing showed that its surface becomes non-uniform. Fig. 1b presents a photograph of the cathode after its use for coating. It can be seen that a region with a rough melted surface is observed along the perimeter of the cathode. In the center, the surface

remains smooth, but cracks appear. The appearance of cracks is not critical from the point of view of further use of the cathode, however, in some cases, cracks can cause its destruction. Such changes on the cathode surface can be associated with the movement of the cathode spot during discharge burning.

a   b

Fig. 1 – Photo of the cathode based on Ti_2AlC MAX phase in the initial state (a) and after its use for vacuum-arc deposition of coatings for 3 h (b)

Another problem arises in the deposition of coatings by ion sputtering, when the cathode is used as a target sputtered with argon ions. It was found that this method also provides a sufficiently high deposition rate of coatings up to 4.5 µm/h. In contrast to the vacuum-arc method, after sputtering the cathode, its surface remains homogeneous without the presence of cracks, however, its composition changes significantly. According to the data of X-ray structural analysis, after sputtering with argon ions ($D_{Ar} = 5 \times 10^{21}$ ions/cm^2) in the surface layer of the cathode, titanium carbide TiC becomes the main phase with a weight content of 46 wt. % The content of Ti_2AlC MAX phase decreases to 26 wt. %. In addition, Ti_3AlC phase appears in the sample (cubic system) with a weight content of 28 wt. %. The change in the phase composition of the target surface after its sputtering indicates an increase in the relative titanium content in it. X-ray fluorescence analysis confirms this result. The atomic ratio of titanium and aluminum in the surface layer of the sputtered target is Ti:Al = 12:1, i.e., the amount of aluminum decreases by 4 times in comparison with the initial state. The change in the elemental composition of the target after sputtering with argon ions is caused by the selective sputtering of Al and C. It is known [20] that during ion sputtering of multicomponent materials containing elements with different atomic masses, predominant sputtering of lighter elements is observed. Intense ion irradiation leads to the decomposition of MAX phases into carbides and the formation of lower compounds [21].

Despite the above-described features of the operation of cathodes based on Ti_2AlC MAX phase, using both deposition methods, coatings were obtained on substrates of titanium alloy Ti6Al4V with a thickness of up to 10 µm. Electron microscopic images of the surface of samples obtained by different methods are shown in Fig. 3. The surface of the coatings is sufficiently smooth, dense and homogeneous without any pores or cracks. The relief of the surface of the ion-plasma coating repeats the relief of the substrate with characteristic scratches from grinding (Fig. 3a). The surface of the vacuum-arc coating has a cellular structure with a cell

size of 5-10 µm (Fig. 3b). The appearance of such a pronounced cellular microrelief on the surface is typical for coatings of nitrides of refractory metals obtained by the method of vacuum-arc deposition [22]. This may be due to the appearance of high compressive internal stresses in the coating plane, which are formed at low bias potentials on the substrate. In the surface layer of the coating, areas with a local loss of shear stability appear, which leads to the formation of a relief on the growth surface.
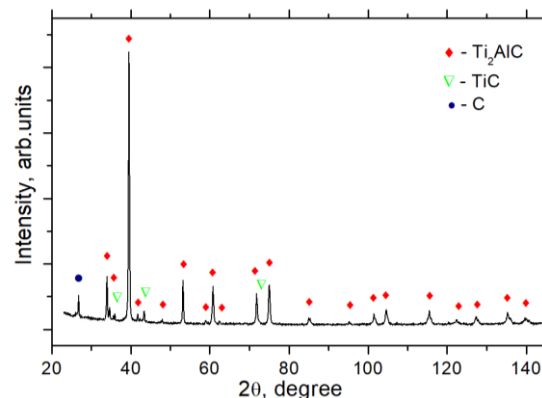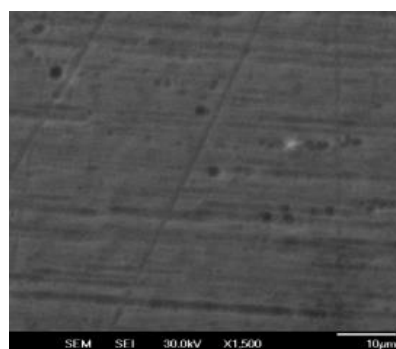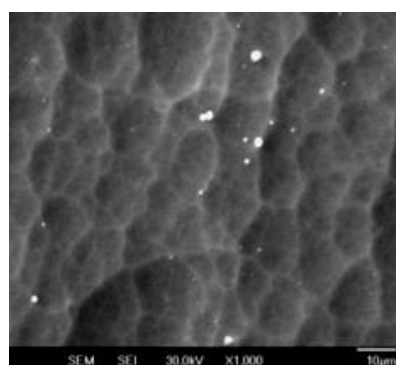

Fig. 2 – Diffraction pattern of the cathode based on Ti_2AlC MAX phase

a

b

Fig. 3 – Electron microscopic images of the surface of coatings obtained by ion sputtering (a) and vacuum-arc deposition (b)

Another feature of vacuum-arc coatings is the presence of a small amount of macroparticles – drops of cathode material. Relatively small droplets up to 1 µm in size are visible both on the surface and in the volume of the coating in the image of its transverse fracture

(Fig. 4). It should be noted that the appearance of a cellular microrelief in films is sometimes caused by their columnar growth, in which the boundaries of the columns appear on the surface. The fracture image clearly shows that in the resulting coating there is no columnar structure, and the average size of structural components in the coating is an order of magnitude smaller than the size of cells on the coating surface.
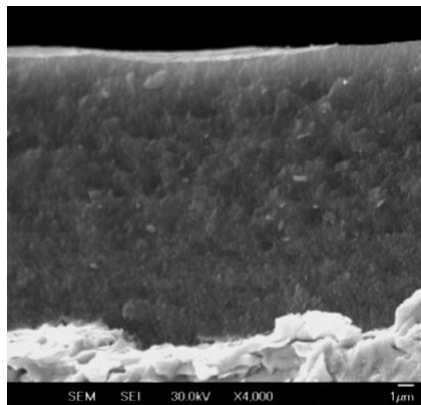

Fig. 4 – Electron microscopic image of a transverse fracture of the sample with the vacuum arc coating

The elemental composition of the coatings was studied by energy dispersive spectroscopy. It was found that chemical elements in the coatings are distributed fairly evenly. Fig. 5 shows maps of the distribution of titanium, aluminum and carbon over the surface and depth of the vacuum-arc coating. The composition of the coatings is shown in Table 1. It can be seen that it somewhat differs from the composition of the cathode. For a coating obtained by ion sputtering, this difference is not very large. The concentrations of aluminum and carbon are only 2 wt. % lower than in the cathode. For a coating obtained by the method of vacuum-arc deposition, this difference is much stronger: the aluminum content decreases sharply in comparison with the cathode. The volume ratio of the components is Ti:Al:C = 9:1:4, which significantly differs from the ratio required for the formation of the stoichiometric composition of Ti_2AlC MAX phase. The fact of the mismatch between the compositions of the cathode and ion-plasma coatings is associated with the difference in the energy and angular distributions of particles generated by the cathode, scattering of particles on the way to the substrate, and selective sputtering of the already deposited coating [23]. The authors of [12], who deposited films by magnetron sputtering of the Ti_2AlC target, showed that the substrate temperature is an important factor determining the concentration of aluminum in condensates. A significant decrease in the aluminum content in the films is observed at high deposition temperatures due to its evaporation. This is consistent with our experiments, since the temperature during deposition of the vacuum-arc coating was significantly higher than that of the coating obtained by ion sputtering.

Fig. 6 shows the diffraction patterns of the obtained coatings, and the results of the phase analysis are given in Table 1. The diffractogram of the coating obtained by ion sputtering reveals rather wide lines of the solid solution (Ti, Al) C based on TiC carbide with a cubic
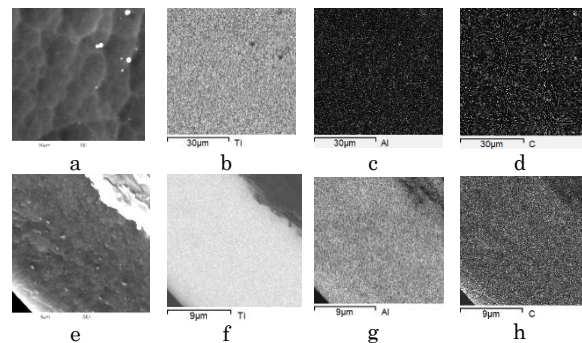

Fig. 5 – SEM images of the surface of the vacuum-arc coating (a), its cross-section (e), and EDX maps of the distribution of elements over the surface (b-d) and in the cross-section (f-h) of the coating

crystal lattice of the NaCl type. No other crystalline phases, including Ti_2AlC MAX phase, were found in the coating, although the composition of the coating does not differ much from that of the cathode. The diffraction pattern of the coating deposited by the vacuum-arc method shows lines of two phases. The main phase, as in the case of ion sputtering, is (Ti, Al) C based on TiC carbide. In addition, the diffraction pattern contains lines of α-Ti with a hexagonal structure. The MAX phase is also not detected in this coating. The ratio of the intensities of the diffraction lines of the detected phases differs from the tabular values, which indicates the presence of texture and makes it impossible to use the obtained data for quantitative phase analysis. The relative intensity of the lines (220) of carbide (Ti, Al) C and (110) α-Ti, located near 60°, is significantly higher than the corresponding values for materials with a chaotic orientation of crystallites. The lines in the diffractogram of this coating are also quite wide, which is due to the small size of coherent scattering regions (CSRs). Indeed, estimates show that the CSR size of the identified phases, regardless of the coating deposition method, is 10-15 nm. It should be noted that, in addition to the identified crystalline phases, the coatings may contain a certain amount of an X-ray amorphous component. This is evidenced by the rather low integral intensity of the revealed reflections and the specific shape of the curves in the diffractograms.

In Fig. 7, diagrams of the penetration of the Berkovich indenter obtained by nanoindentation of the samples are shown. The implantation diagram of the cathode material based on Ti_2AlC MAX phase was obtained at a load of up to 180 mN (Fig. 7a). Its feature is the presence of steps on the loading curve. At the initial stage of deformation, a monotonic increase in the penetration depth is observed with an increase in the load. When the load reaches a value of ~ 40 mN, an abrupt increase in strain occurs: a sharp increase in the indentation depth by ~ 25 nm in a fraction of a second (pop-in) is observed, after which a smooth growth continues. A similar situation is repeated three more times when the load reaches 80, 110 and 140 mN, and with each jump, the strain increment increases, reaching 60 nm. The formation of steps in the nanoindentation diagrams of MAX phases is associated with the appearance of cracks or bending bands in the layered structure under load [24].

Table 1 – Results of elemental and phase analysis of the cathode and coatings

| Sample	Preparation method	Composition, wt. %	Revealed phases	Structural type	Lattice parameters, nm	
					a	*c*
Cathode	Hot pressing	$Ti_{0.54}Al_{0.19}C_{0.27}$	Ti_2AlC (basic)	194 : $P6_3$/mmc	0.3048	1.3639
			C	194 : $P6_3$/mmc	0.2464	0.6657
			TiC	225 : Fm3m	0.4330	
Coating	Vacuum arc deposition	$Ti_{0.65}Al_{0.07}C_{0.28}$	(Ti, Al) C (basic)	225 : Fm3m	0.4299	
			α-Ti	194 : $P6_3$/mmc	0.2936	0.4558
	Ion sputtering	$Ti_{0.58}Al_{0.17}C_{0.25}$	(Ti, Al)C	225 : Fm3m	0.4352	
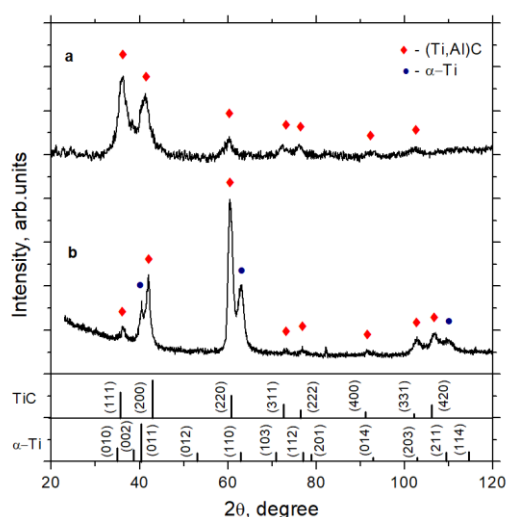
Fig. 6 – Diffraction patterns of the coatings obtained with a cathode based on Ti_2AlC MAX phase by ion sputtering (a) and vacuum arc deposition (b)

Steps are not observed in the indenter penetration diagrams for coatings. As an illustration, Fig. 7b shows a diagram of the penetration of the Berkovich indenter obtained by nanoindentation of a vacuum-arc coating. The maximum load of 75 mN is chosen so that the penetration depth of the indenter does not exceed 10 % of the coating thickness, which makes it possible to exclude the influence of the substrate on the results of nanoindentation. There are no features in the diagram for the coating, and in the entire interval there is a monotonic increase in the penetration depth with increasing load.

Based on the results of processing the nanoindentation diagrams, the values of Young's modulus (*E*) and hardness (*H*) of the samples were determined, which are shown in Table 2. The table also shows the values of the *H*/*E* parameter, which is often used to characterize the resistance of a material to elastic deformation of fracture. Wear-resistant coatings require a combination of strength, hardness and recoverability. The combination of high hardness and low modulus of elasticity, i.e., higher *H*/*E* values, are considered optimal for ensuring high wear resistance, especially in difficult processes associated with shock loads and erosion. The cathode based on Ti_2AlC MAX phase has a hardness of 10 GPa and a Young's modulus of 238 GPa. The *H*/*E* ratio is 0.04, which is typical for coarse crystalline materials. The hardness of the cathode is more than two times
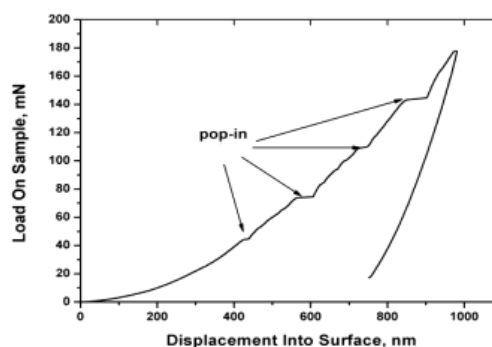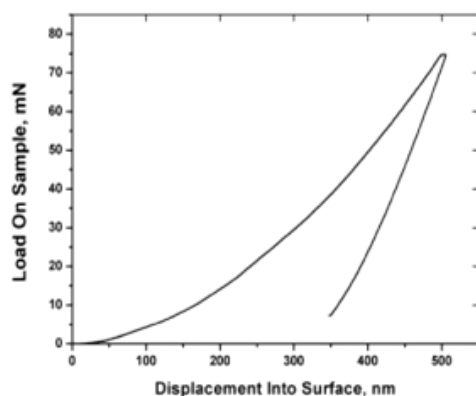

Fig. 7 – Diagrams of the penetration of the Berkovich indenter obtained by nanoindentation of the cathode material based on Ti_2AlC MAX phase (a) and a vacuum-arc coating obtained with its help (b)

higher than the values given in the literature for Ti_2AlC MAX phase [3], which is mainly due to the influence of solid inclusions of titanium carbide TiC. According to the literature data, the hardness of TiC reaches 32 GPa [3].

The hardness of the obtained coatings is higher than that of the cathode. The coating, deposited by the method of ion sputtering, having in its composition a single crystalline phase (Ti, Al) C, has a hardness of 21 GPa. The hardness of the vacuum-arc coating is lower and equals 13 GPa, which is most likely due to the presence of α-Ti in its composition. At the same time, the *H*/*E* ratio of the coatings is significantly higher than that of the cathode, reaching values of 0.06-0.07, which is typical for wear-resistant coatings with a nanocrystalline structure.

Table 2 – Results of nanoindentation of the cathode material and coatings

Sample	Manufacturing method	Composition, wt. %	H, GPa	E, GPa	H/E
Cathode	Hot pressing	$Ti_{0.54}Al_{0.19}C_{0.27}$	10	238	0.04
Coating	Vacuum-arc deposition	$Ti_{0.65}Al_{0.07}C_{0.28}$	13	233	0.06
	Ion sputtering	$Ti_{0.58}Al_{0.17}C_{0.25}$	21	293	0.07
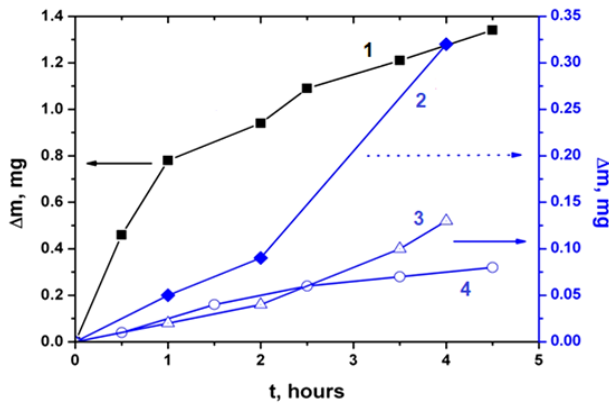
Fig. 8 – Kinetic curves of cavitation wear of samples: 1 – cathode material based on Ti_2AlC MAX phase; 2 – substrate made of titanium alloy Ti6Al4V without coating; 3 – TiN coated substrate; 4 – substrate with vacuum-arc coating $Ti_{0.65}Al_{0.07}C_{0.28}$

The results of cavitation tests of the samples are illustrated in Fig. 8. Kinetic curves of cavitation wear of the cathode material based on Ti_2AlC MAX phase and the vacuum-arc coating made with this cathode on the substrate of titanium alloy Ti6Al4V are shown.

The vacuum-arc coating was selected for testing because its hardness is close to that of the cathode. Also, for comparison, Fig. 8 shows the wear of the substrate without coating and with a TiN coating, which is widely used for hardening and protecting the surface of titanium alloys [25]. It is seen that the cathode has an extremely low cavitation resistance. The cavitation wear of the cathode in 4 h of testing reaches 1.3 mg, which is 4 times higher than the wear of titanium alloy Ti6Al4V. The deposition of vacuum-arc coatings makes it possible to further increase the surface resistance of Ti6Al4V alloy. The wear of the surface of both samples with coatings after 2.5 h of cavitation tests does not exceed 0.07 mg. Then, the wear of $Ti_{0.65}Al_{0.07}C_{0.28}$ coating made with the MAX phase cathode is slowed down compared to the TiN coating. The average wear rate of vacuum-arc coating $Ti_{0.65}Al_{0.07}C_{0.28}$ is 0.02 mg/h, which is 1.5 times lower than that of TiN coatings, 3 times lower than that of an uncoated alloy.

A feature of the kinetics of cathode wear is rapid destruction at the initial stage of testing. In the first hour, the sample loses 0.8 mg. Then the rate of cavitation wear decreases to 0.15 mg/h. The unexpectedly low wear resistance of the cathode material can be due to the layered crystal structure of Ti_2AlC MAX phase. Carbide blocks under the action of receiving load can be easily chipped along the metal layers. At the initial stage of wear, this occurs especially quickly in sufficiently large grains, which are favorably oriented with respect to the surface of the specimen by the planes of easy cleavage. This possibility is absent in nanostructured carbide coatings.

4. CONCLUSIONS

The structure, mechanical properties and cavitation resistance of the material based on Ti_2AlC MAX phase, as well as ion-plasma coatings deposited using these cathodes, have been investigated.

It was found that the cathode material contains 83 wt. % Ti_2AlC MAX phase. Ti_2AlC MAX phase is characterized by a high hardness of 10 GPa, an H/E value of 0.04 and a low cavitation resistance. The average cavitation wear of the cathode is 4 times higher than that of titanium alloy Ti6Al4V.

Using cathodes based on Ti_2AlC MAX phase on substrates of titanium alloy Ti6Al4V, nanocrystalline carbide coatings were obtained by two methods such as vacuum-arc deposition and ion sputtering with an arc gas plasma source. The elemental and phase composition of the obtained coatings differs from that of the cathode. Ti_2AlC MAX phase was not found in the coatings. $Ti_{0.58}Al_{0.17}C_{0.25}$ coating, deposited by the method of ion sputtering, having in its composition a single crystalline phase – cubic (Ti, Al) C, is characterized by a hardness of ~ 21 GPa. The hardness of the vacuum-arc coating $Ti_{0.65}Al_{0.07}C_{0.28}$ is closer to the hardness of the cathode and is ~ 13 GPa, which is associated with the presence of two phases in its composition: (Ti, Al) C and a-Ti. For coatings, the ratio H/E = 0.06-0.07, which is 1.5 times higher than that of the cathode. The average rate of cavitation wear of the vacuum-arc coating $Ti_{0.65}Al_{0.07}C_{0.28}$ is 1.5 times lower than that of the TiN coating and 3 times lower than that of the uncoated Ti6Al4V alloy.

The data obtained indicate that the use of cathodes based on MAX phases is promising for the synthesis of protective ion-plasma coatings on titanium alloys.

REFERENCES

1. Jesus Gonzalez-Julian, *J. Am. Ceram. Soc.* **00**, 1 (2020).
2. A. Li, C. Hu, M. Li, Y. Zhou, *J. Eur. Ceram. Soc.* **29**, 12 (2009).
3. X.H. Wang, Y.C. Zhou, *J. Mater. Sci. Technol.* **26**, 5 (2010).
4. N.V. Tzenov, M.W. Barsoum. *J. Am. Ceram. Soc.* 83, 825, (2000).
5. W.B. Zhou, B.C. Me, J.Q. Zhu, X.L. Hong, *J. Mater. Sci.* **40**, 2099 (2005).

6. A.V. Starostina, T.A. Prikhna, M.V. Karpets, S.N. Dub, P. Chartier, T. Cabiosh, V.B. Sverdun, V.E. Moshchil', A.V. Kozyrev, *J. Superhard Mater.* **33**, 307 (2011).
7. O. Berger, *Surface Eng.* **36**, 3 (2020).
8. Y. Li, G. Zhao, Y. Qian, J. Xu, M. Li, *Vacuum* **153**, 62 (2018).
9. C. Tang, M. Klimenkov, U. Jaentsch, H. Leiste, M. Rinke, S. Ulrich, M. Steinbruck, HJ Seifert, M. Stueber, *Surf. Coat. Technol.* **309**, 445 (2017).

10. O. Wilhelmsson, J.-P. Palmquist, T. Nyberg, U. Jansson, *Appl. Phys. Lett.* **85**, 1066 (2004).
11. W. Garkas, C. Leyens, A. Flores-Renteria, *Adv. Mater. Res.* **89-91**, 208 (2010).
12. J. Frodelius, P. Eklund, M. Beckers, POÅ. Persson, H. Högberg, L. Hultman, *Thin Solid Films* **518**, 6 (2010).
13. C. Walter, C. Martinez, T. EI-Raghy, JM Schneider, *Steel Research Int.* **76**, 225 (2005).
14. T.O. Prikhna, V.Ya. Podhurs'ka, O.P. Ostash, B.D. Vasyliv, V.B. Sverdun, M.V. Karpets, T.B. Serbenyuk, *Mater. Sci.* **55**, 1 (2019).
15. Yu.V. Kovtun, A.S. Kuprin, V.M. Lunev, *Probl. At. Sci. Tech.* **1**, 145 (2019).
16. A.S. Kuprin, T.A. Prikhna, E.N. Reshetnyak, M.A. Bortnitskaya, I.V. Kolodiy, V.A. Belous, S.N. Dub, A.V. Ilchenko, V.B. Sverdun, *J. Nano- Electron. Phys.* **12**, 5 (2020).
17. WC Oliver, GM Pharr, *J. Mater. Res.* **19**, 3 (2004).
18. V.G. Marinin, V.I. Kovalenko, N.S. Lomino, Yu.A. Zadneprovsky, V.D. Ovcharenko, *Int. Symposium on Discharges and Electrical Insulation in Vacuum, ISDEIV.* **2**, 567 (2000).
19. ASTM G32-16, *Standard Test Method for Cavitation Erosion Using Vibratory Apparatus*, (ASTM International: West Conshohocken: PA: 2016).
20. V.S. Smentkowski *Progr. Surf. Sci.* **64**, 1 (2000).
21. J. Ward, S. Middleburgh, M. Topping, A. Garner, D. Stewart, M.W. Barsoum, M. Preuss, P. Frankel, *J. Nucl. Mater.* **502**, 220 (2018).
22. T. Kuznetsova, V. Lapitskaya, A. Khabarava, S. Chizhik, B. Warcholinski, A. Gilewicz, A. Kuprin, S. Aizikovich, B. Mitrin, *Nanomaterials* **10** 2361 (2020).
23. I.I. Aksenov, V.A. Belous, Yu.A. Zadneprovskiy, A.S. Kuprin, N.S. Lomino, V.D. Ovcharenko, O.V. Sobol, *24th ISDEIV*, 497 (2010).
24. M.W. Barsoum, M. Radovic, *Annu. Rev. Mater. Res.* **41**, 195 (2011).
25. V.A. Belous, V.N. Voevodin, V.M. Khoroshikh, G.I. Nosov, V.G. Marinin, S.A. Leonov, V.D. Ovcharenko, V.I. Kovalenko, A.A. Komar, A.S. Kuprin, L.O. Shpagina, *Sci. Innov.* **12**, 4 (2016).

Структура та механічні характеристики катодів з МАХ фази Ti₂AlC та осаджених іонно-плазмових покриттів

М.О. Бортницька[1], О.М. Решетняк[1], О.С. Купрін[1], Т.О. Пріхна[2], В.Б. Свердун[2], І.В. Колодій[1], В.А. Білоус[1], В.Г. Марінін[1]

[1] *Національний Науковий Центр "Харківський Фізико-технічний Інститут", вул. Академічна 1, 61108 Харків, Україна*
[2] *Інститут Надтвердих Матеріалів імені В.М. Бакуля Національної Академії Наук України, вул. Автозаводська 2, 04074 Київ, Україна*

У роботі вивчені характеристики структури, твердості, пружності та кавітаційної стійкості матеріалу катодів на основі МАХ фази Ti₂AlC, виготовлених методом гарячого пресування, а також іонно-плазмових покриттів, осаджених з використанням цих катодів на титановий сплав Ti6Al4V. Встановлено, що матеріал катода, який містить 83 ваг. % МАХ фази Ti₂AlC, характеризується твердістю 10 ГПа, значенням параметра *H*/*E* 0,04 і низькою кавітаційною стійкістю. Середній кавітаційний знос катоду у 4 рази вище, ніж знос титанового сплаву Ti6Al4V. З'ясовано, що елементний і фазовий склад осаджених покриттів відрізняється від складу катода. Основною фазою в покриттях є нанокристалічний карбід (Ti, Al) C з кубічною структурою типу NaCl. Покриття $Ti_{0,58}Al_{0,17}C_{0,25}$, осаджене методом іонного розпилення за допомогою дугового джерела газової плазми, характеризується твердістю 21 ГПа. Твердість вакуумно-дугового покриття $Ti_{0,65}Al_{0,07}C_{0,28}$ ближче до твердості катоду – 13 ГПа, що пов'язано з наявністю в його складі α-Ti. Співвідношення *H*/*E* у покриттів в 1,5 рази вище, ніж у катода, що є передумовою високої кавітаційної стійкості. Середня швидкість кавітаційного зношування вакуумно-дугового покриття $Ti_{0,65}Al_{0,07}C_{0,28}$ у 1,5 рази нижче, ніж вакуумно-дугового покриття TiN і в 3 рази нижче, ніж сплаву Ti6Al4V без покриття.

Ключові слова: МАХ фаза, Покриття, Вакуумно-дугове осадження, Іонне розпилення, Наноіндентування, Кавітаційний знос.